

Supporting information

Flexible and shape-reconfigurable hydrogel interlocking adhesives for high adhesion in wet environments based on anisotropic swelling of hydrogel microstructures

Hyun-Ha Park,[†] Minho Seong,[†] Kahyun Sun,[†] Hangil Ko,[†] Sang Moon Kim,[‡] and Hoon Eui Jeong^{*,†}

[†]Department of Mechanical Engineering, Ulsan National Institute of Science and Technology (UNIST), Ulsan 44919, Republic of Korea

[‡]Department of Mechanical Engineering, Incheon National University, Incheon 22012, Republic of Korea

*Corresponding author email: hoonejeong@unist.ac.kr

Experimental section

Fabrication of the reconfigurable hydrogel microhook array

A silicon wafer was first baked at 70 °C for 10 min in a convection oven for dehydration. A lift-off resist (LOR30B, Microchem, USA) was then spin-coated on the wafer at 1000 rpm for 30 s, followed by baking at 220 °C for 25 min. This LOR coating process was repeated once again to obtain a thick LOR layer. Subsequently, a positive photoresist (AZ4330, Microchem, USA) was spin-coated on the LOR layer at 1000 rpm for 30 s, followed by baking at 90 °C for 90 s. The wafer was then exposed to UV light ($\lambda = 365$ nm, dose = 50 mJ cm⁻²) with a photomask having a microhole pattern, followed by UV-ozone (UVO) exposure for 20 s. Subsequently, the UV-exposed AZ photoresist and the LOR layers were developed using a developer (AZ 300 MIF, AZ Electronics Materials Corp, USA) for 5 min. Finally, the Si master was rinsed with DI water and blow-dried with nitrogen. For surface hydrophobization, the master was treated with a fluorinated self-assembled monolayer (SAM) solution (trichloro(1H,1H,2H,2H-perfluorooctyl)silane from Sigma Aldrich, USA). A 10:1 (w/w) mixture of the poly(dimethylsiloxane) (PDMS) (Sylgard 184, Dow Corning, USA) precursor and curing agent was poured onto the surface-treated Si master to generate a negative replica of the Si master, followed by thermal curing at 70 °C for 2 h. The cured PDMS replica was removed from the master, resulting in a negative replica of the Si master. Drops of PEGDMA (MW ~550 from Sigma Aldrich, USA) with 0.2 wt.% of photo-initiator (2-hydroxy-2-methylpropiophenone from Sigma Aldrich, USA) were then drop-dispensed onto the replicated PDMS mold, and a 250 μ m-thick polyethylene terephthalate (PET) film was slightly pressed against the PEGDMA drop, followed by subsequent UV exposure ($\lambda = 365$ nm, dose = 200 mJ cm⁻²) and removal from the PDMS mold. The resulting PEGDMA samples were additionally exposed to UV for several hours for complete curing by removal of the trapped polymer radicals and unsaturated acrylates.

Imaging of the hydrogel microhook array

Confocal microscopy images of the fabricated PEGDMA samples were obtained using a multi-photon confocal microscope (LSM 780 Configuration 16 NLO, Carl Zeiss, Germany). PEGDMA added with rhodamine B was used to fabricate the PEGDMA samples for confocal

imaging. High-resolution scanning electron microscopy (SEM) images of the PEGDMA microstructures were obtained using a HITACHI S-4800 microscope (Hitachi, Japan). The samples were coated with a Pt layer (~5 nm thick) by metal sputtering (K575X sputter coater, Quorum Emitech, UK) to avoid the charging effects.

Surface characterization

The contact angles (CAs) of the water droplets on the planar PEGDMA film were measured using a drop shape analyzer (SDLAB 200TEZD, FEMTOFAB, Korea) at room temperature. The measurement for each sample was repeated five times at random positions on the specimen to average the CA. AFM (Multimode V, Veeco) images of the planar PEGDMA samples were recorded in the tapping mode at a scan rate of 1.0 Hz and a scan resolution of 256×256 pixels.

Attenuated total reflectance-Fourier transform infrared spectroscopy

Fourier transform infrared spectroscopy was performed on a Cary 670 (Agilent) instrument with a Ge 45° single reflection attenuated total reflectance crystal (PIKE MIRacle, Germany). The spectra were recorded using Agilent resolution software with an average of 32 scans in the wavenumber range of $650\text{--}4000\text{ cm}^{-1}$ at a 4 cm^{-1} resolution.

Adhesion measurements

The pull-off and shear forces in the interlocked samples were evaluated using a custom-built equipment (Figure S2). The equipment consisted of motorized movable parts along the horizontal and vertical directions connected with load cells (KTOYO, Korea) and a stage for mounting the samples. The adhesion strengths were measured by bringing the upper and lower surfaces ($10\text{ mm} \times 10\text{ mm}$) of the PEGDMA microhook arrays into contact with a controlled preload of $\sim 10\text{ N cm}^{-2}$ and interlocking with each other using the equipment. An in-plane strain was then applied by the motorized parts until separation occurred. The load

cells connected to the movable parts recorded the adhesive force in the normal and shear directions. For the wet adhesion tests, the interlocked samples were submerged in a small water bath placed on the adhesion test equipment for a specific time, followed by the pull-off and shear measurements. The pull-off and shear measurements were conducted 10 times for each sample, and the averaged value was used (the error bars in the graph indicate a standard deviation). Meanwhile, for the durability tests, the interlocked samples were swollen in the water bath for specific times (i.e., 10 min and 10 h), followed by adhesion measurements under wet conditions. The interlocked samples were then dried on a hot plate at 30 °C, and the adhesion strengths of the dried samples were re-measured. The shear and normal interlocking adhesion measurements were repeated during 10 times of repeated swelling and deswelling cycles (Figure S4).

Measurements of Young's modulus

Young's moduli and elongations at break of the PEGDMA samples in the dry and swollen states (in water after 20 h of exposure) were determined by a universal testing machine (UTM, Instron 5982, Instron Corporation, USA) analysis. Testing was performed under ASTM D638 mode, and the stretching rate was 10 mm/min. The typical sample dimension was 150 × 15 × 5 (length × width × thickness, mm). The measurements were conducted five times for each sample, and the averaged value was used.

Preparation of the PEGDMA surfaces with roughness

A PEGDMA film with roughness similar to that of the swollen PEGDMA film (RMS: ~0.794 nm) was prepared to examine the effect of the RMS on the adhesion strength by replicating a Si wafer with roughness with the PEGDMA. The Si wafer with roughness was prepared by exposing the bare Si wafer to oxygen plasma for 220 s (50 sccm, power: 200 W). The resulting PEGDMA film had an RMS of ~0.77 nm, as shown in Figure S10. The adhesion of the prepared PEGDMA film was measured by bringing two identical PEGDMA films into contact with each other.

Theoretical analysis of the interlocking adhesion strength

A. Normal interlocking force

We derived a theory based on a force balance among the microhook arrays to gain further understanding on the interlocking behaviors of the fastener. The normal interlocking adhesion force can be given as follows from a force equilibrium for a single paired interlocked microhook array:

$$F_{normal} = nF_{ext} = n(F_{b,t} + \frac{1}{3}F_{ad} + f_1 + f_2) \quad (S1)$$

where n is the number of microhooks per unit area ($1 \times 1\text{cm}^2$); F_{ext} is the external force acting on the single microhook; $F_{b,t}$ is the bending force acting on the tip; F_{ad} is the adhesion force between the tip and the bottom substrate; and f_1 and f_2 are the frictional forces between the side walls of the stem and the tip of the interlocked microhooks, respectively (Figures S6a and S6b). The approximated bending force ($F_{b,t}$) acting on the tip can be derived as follows by assuming the tip as a simple rectangular beam (Figure S7 and Eqs. (S1*)–(S2*)):

$$F_{b,t} = h_t^2 \sigma_u \sqrt{\frac{4r_t^2}{3p^2} - \frac{1}{9}} \quad (S2)$$

where σ_u is the ultimate tensile strength of the material; h_t is the tip thickness; r_t is the tip radius; and p is the center-to-center pitch of the array. The adhesion force (F_{ad}) for the dry conditions can be obtained by considering the van der Waals interaction between the tip and the substrate (Eq. (S3a)), while a capillary interaction needs to be added for the wet conditions (Eq. (S3b)) (see Eq. (S5*)):

$$F_{ad} = \begin{cases} F_{vdw,flat} = \frac{Ar_c^2}{6(h_s - h_t)^3} & \text{(for dry) (S3a)} \\ F_{vdw,flat} + F_{cap,flat} = \frac{Ar_c^2}{6(h_s - h_t)^3} + \pi\gamma r_c \left(1 + \frac{2r_c \cos\theta_{CA}}{h_s - h_t}\right) & \text{(for wet) (S3b)} \end{cases}$$

where $F_{vdw,flat}$ and $F_{cap,flat}$ represent the van der Waals force and the capillary force between the tip and the substrate, respectively; A is the hamaker constant ($\sim 5 \times 10^{-20}$ and $\sim 0.5 \times 10^{-20}$ for the dry and wet conditions, respectively)¹; r_c is the radius of contact between the tip and the substrate ($\sim 8.9 \mu\text{m}$ and $\sim 6.8 \mu\text{m}$ each for the dry and wet conditions from Figures 2e and f,

respectively); h_s is the stem height of the structure; γ is the surface tension of water; and θ_{CA} ($\sim 40^\circ$) is the water contact angle on the PEGDMA film. The frictional forces (f_1 and f_2) were also dependent on the dry and wet conditions:

$$f_1 = f_2 = f$$

$$= \begin{cases} \mu F_{vdw,cyl} = \frac{\mu A h_t}{8\sqrt{2}D_1^{5/2}} \sqrt{\frac{r_s r_t}{r_s + r_t}} \quad (\text{for dry}) \quad (\text{S4a}) \\ \mu(F_{vdw,cyl} + F_{cap,cyl}) = \mu \left[\frac{\mu A h_t}{8\sqrt{2}D_1^{5/2}} \sqrt{\frac{r_s r_t}{r_s + r_t}} + \pi \gamma \frac{h_t}{2} \left(1 + \frac{h_t \cos \theta_{CA}}{\frac{p}{\sqrt{3}} - r_s - r_t} \right) \right] \quad (\text{for wet; } D_1 > 0.4 \text{ nm}) \quad (\text{S4b}) \end{cases}$$

where μ is the static coefficient of friction at the interface (~ 0.12 and ~ 0.08 for the dry and wet conditions, respectively)²; and $F_{vdw,cyl}$ and $F_{cap,cyl}$ are the van der Waals force and the capillary force between the side walls of the stem and the tip of the microhooks, respectively (see Eqs. (S6*)–(S8*) and (S10*) for details). According to Eq. (S4b), wet friction must be considered when the arrays are swollen by water. However, when the microhook arrays are interlocked very tightly, and the gap between the microhooks is very small ($D_1 \leq D_0 = 0.4$ nm, where D_0 is the cut-off gap distance),¹ the $\mu F_{cap,cyl}$ can be ignored as the friction corresponds to the boundary lubrication regime.³ The approximated normal adhesion strength for the dry and wet conditions can be obtained as follows by applying Eqs. (S2)–(S4) into Eq. (S1) and considering the dominant terms:

$$F_{normal} \cong \begin{cases} nF_{b,t} = n h_t^2 \sigma_u \sqrt{\frac{4r_t^2}{3p^2} - \frac{1}{9}} \quad (\text{for dry}) \quad (\text{S5a}) \\ n \left(F_{b,t} + \frac{1}{3} F_{cap,flat} \right) = n \left[h_t^2 \sigma_u \sqrt{\frac{4r_t^2}{3p^2} - \frac{1}{9}} + \frac{1}{3} \pi \gamma r_c \left(1 + \frac{2r_c \cos \theta_{CA}}{h_s - h_t} \right) \right] \quad (\text{for wet}) \quad (\text{S5b}) \end{cases}$$

B. Shear interlocking force

The shear adhesion force (F_{shear}) can be written as follows based on a force balance for the single paired interlocked microhook array (Figures S6c and d):

$$F_{shear} = n F_{ext} \cos(\theta_{ext}) = n \left[F_x \cos\left(\frac{\pi}{2} - \theta_m\right) + F_y \cos(\theta_m) \right] \quad (\text{S6})$$

where θ_{ext} is the angle of the external force from a horizontal surface; θ_m is the tilting angle of the microhook; and F_x and F_y are the x and y components of the external force, respectively (Figure S6d):

$$F_x = \frac{1}{3} (F_{b,m} + f_3 + f_4) = \frac{1}{3} (F_{b,m} + \mu F_{b,t} + \mu F_{vdw,tip} + \mu F_{vdw,flat}) \quad (\text{S7a})$$

$$F_y = \frac{1}{3}(F_{b,t} + F_{vdw,flat} + f_1 + f_2) = \frac{1}{3}(F_{b,t} + F_{vdw,flat} + 2\mu F_{vdw,cyl} + \mu F_{b,m}) \quad (S7b)$$

where $F_{b,m}$ is the bending force acting on the microhook; $f_1, f_2, f_3,$ and f_4 are the frictional forces at each interface shown in Figure S6b; and $F_{vdw,tip}$ is the van der Waals force between the tip bottoms of the interlocked array. For a simplified modeling, we assumed that when a shear load is applied to the swollen microhook array, each microhook undergoes a compressive stress by the shear load, resulting in an increase in the structural height because of the Poisson's ratio (Figure S6d). Subsequently, the gap between the tip and the substrate would be very small, enabling the exclusion of the term of the capillary friction in Eq. (S7), as described earlier.³ $F_{b,m}$ and $F_{vdw,tip}$ can be given as follows by assuming the microhook as a simple cylinder (Figures S8–9 and Eqs. (S3*)–(S5*)):

$$F_{b,m} = \frac{\pi \left(\frac{r_s + r_t}{2}\right)^3}{4 \left(h_s + \frac{h_t}{2}\right)} \sigma_u \quad (S8)$$

$$F_{vdw,tip} = \frac{A}{6\pi D_t} \left(2\theta r_t^2 - P \sqrt{\frac{r_t^2}{3} - \frac{p^2}{36}} \right) \quad (S9)$$

where D_t is the distance between two facing surfaces of the tips, and θ is the angle between the horizontal line and the intersecting point formed by the two overlapped circular tips (Figure S9). The shear force can be approximately given as follows by plugging Eqs. (7)–(9) into Eq. (6) and considering dominant terms:

$$F_{shear} \cong \begin{cases} \frac{n}{3} (F_{b,m} + \mu F_{vdw,tip}) \cos\left(\frac{\pi}{2} - \theta_m\right) & \text{(for dry)} \quad (S10a) \\ \frac{n}{3} (F_{b,m} + \mu F_{vdw,flat} + \mu F_{vdw,tip}) \cos\left(\frac{\pi}{2} - \theta_m\right) & \text{(for wet)} \quad (S10b) \end{cases}$$

Figure S6e and S6f shows the plot of the measured shear and normal adhesion forces of the interlocked array with different pitches. The geometrical parameters of 20 h-swollen arrays were utilized for the wet adhesion calculation (Figure 2f). Interestingly, the experimental results agreed well with the theoretical predictions (Figure S6e and S6f), demonstrating the validity of our simple analytical models.

C. Derivations of the individual force components

(i) Bending force acting on the tip of the microhooks ($F_{b,t}$) and the microhook (F_m)

The circular tip was considered as a simple rectangular beam (Figure S7) for a simplified analytical analysis of the bending force of tip ($F_{b,t}$). The ultimate tensile strength for the rectangular beam can be expressed as⁴:

$$\sigma_u = \frac{M \frac{h_t}{2}}{I} = \frac{F_{b,t}}{h_t^2 \sqrt{\frac{4r_t^2}{3p^2} - \frac{1}{9}}} \quad (\text{S1}^*)$$

where M is the bending moment ($M = \frac{p}{2\sqrt{3}} F_{b,t}$), and I is the second moment of inertia ($I = \frac{bh_t^3}{12} = \frac{h_t^3}{36} \sqrt{36r_t^2 - 3p^2}$) of the beam. Consequently, $F_{b,t}$ can be obtained as:

$$F_{b,t} = h_t^2 \sigma_u \sqrt{\frac{4r_t^2}{3p^2} - \frac{1}{9}} \quad (\text{S2}^*)$$

The microhook was considered as a simple circular cylinder for a simplified analytical solution of the bending force of the microhook ($F_{b,m}$) (Figure S8). The ultimate tensile strength of the cylinder is expressed as follows:

$$\sigma_u = \frac{M \left(\frac{r_s + r_t}{2} \right)}{I} = \frac{F_{b,m} \left(h_s + \frac{h_t}{2} \right)}{\frac{\pi \left(\frac{r_s + r_t}{2} \right)^3}{4}} \quad (\text{S3}^*)$$

where M is the bending moment ($M = F_{b,m} \left(h_s + \frac{h_t}{2} \right)$), and I is the second moment of inertia ($I = \frac{\pi \left(\frac{r_s + r_t}{2} \right)^4}{4}$) of the cylinder. Consequently, $F_{b,m}$ can be obtained as:

$$F_{b,m} = \frac{\pi \left(\frac{r_s + r_t}{2} \right)^3}{4 \left(h_s + \frac{h_t}{2} \right)} \sigma_u \quad (\text{S4}^*)$$

(ii) van der Waals force between the surfaces ($F_{vdw,flat}$, $F_{vdw,tip}$, and $F_{vdw,cyl}$)

The van der Waals force between the two flat surfaces is given as¹:

$$F_{vdw} = \frac{A}{6\pi D^3} A_c \quad (\text{S5}^*)$$

where A is the hamaker constant; D is the distance; and A_c is the contact area between the surfaces. The van der Waals forces at the interfaces of the tip/substrate ($F_{vdw,flat}$) and of the tip/tip ($F_{vdw,tip}$) be expressed as Eqs. (S3a) and (S9), respectively, by applying A_c into Eq. (S5*).

The van der Waals force between the side walls of the circular cylinder is given as¹:

$$F_{vdw} = \frac{Al}{8\sqrt{2}D^{5/2}} \sqrt{\frac{r_1 r_2}{r_1 + r_2}} \quad (S6^*)$$

where l is the contact length, and r_1 and r_2 are the radii of the cylinders in contact.

Consequently, one can have $F_{vdw,cyl}$ as follows:

$$F_{vdw,cyl} = \frac{Ah_t}{8\sqrt{2}D_1^{5/2}} \sqrt{\frac{r_s r_t}{r_s + r_t}} \quad (S7^*)$$

(iii) Capillary adhesion force between surfaces ($F_{cap,flat}$ and $F_{cap,cyl}$)

The capillary-mediated adhesion between the two surfaces is given as⁵:

$$F_{cap} = \pi\gamma R \left(1 + \frac{2R\cos\theta_{CA}}{h} \right) \quad (S8^*)$$

where γ is the surface tension of water; R is the contact radius; h is the distance between the surfaces; and θ_{CA} is the contact angle of water on the surface. Using Eq. (S8^{*}), the capillary adhesion at the tip/substrate and the side walls of stem/tip are given by Eqs. (S9^{*}) and (S10^{*}) as follows, respectively:

$$F_{cap,flat} = \pi\gamma r_c \left(1 + \frac{2r_c\cos\theta_{CA}}{h_s - h_t} \right) \quad (S9^*)$$

$$F_{cap,cyl} = \pi\gamma \frac{h_t}{2} \left(1 + \frac{h_t\cos\theta_{CA}}{\frac{p}{\sqrt{3}} - r_s - r_t} \right) \quad (S10^*)$$

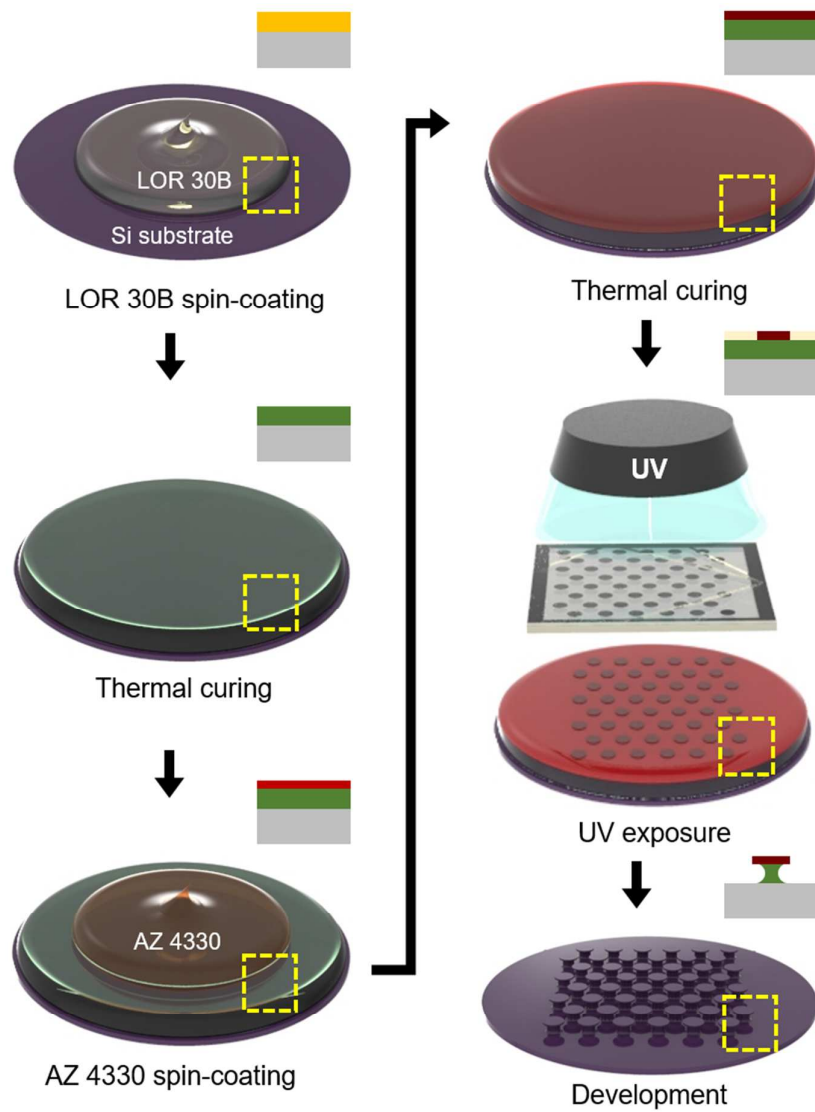


Figure S1. Fabrication procedure of the master with the positive microhook arrays by photolithography using two layers of the photoresist (i.e., LOR30B and AZ 4330).

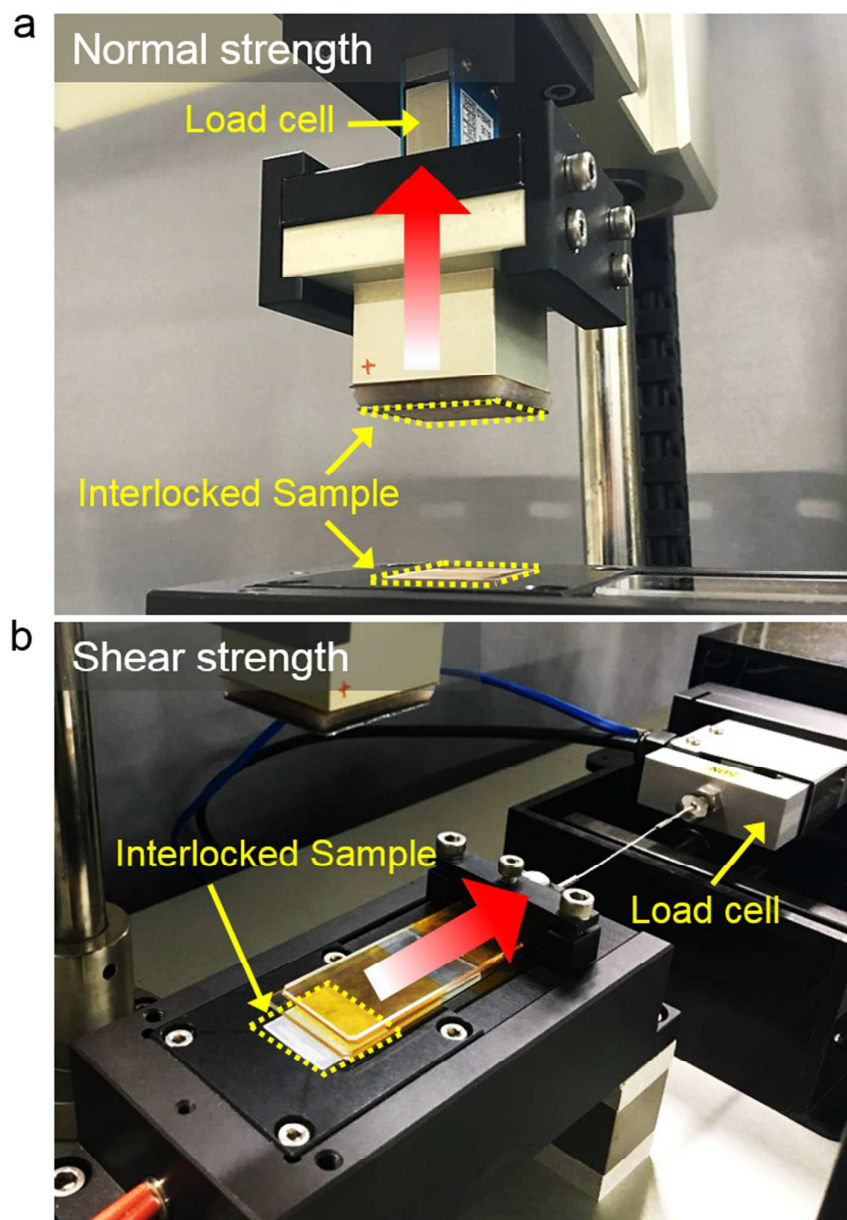


Figure S2. Photographs of the custom-built equipment used for the adhesion measurement tests: set-up for the measurements of the (a) normal adhesion and (b) shear strengths.

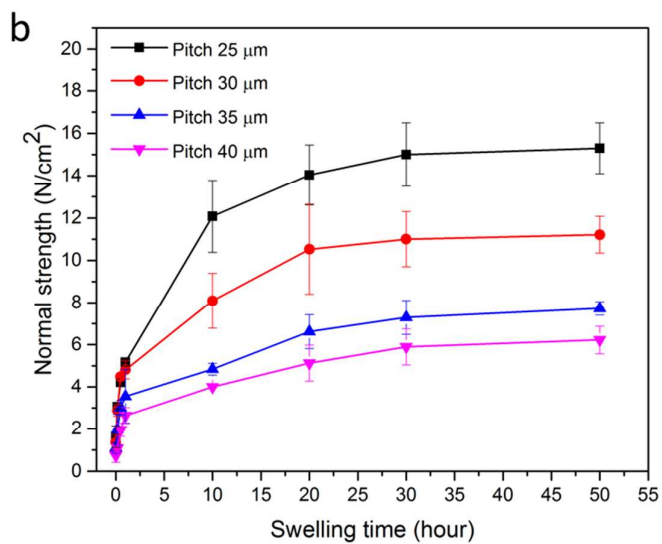
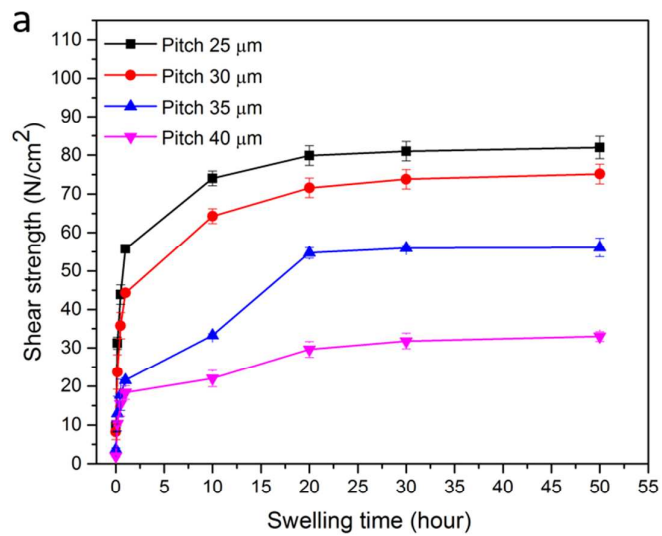


Figure S3. (a) Shear and (b) normal interlocking adhesion strengths of the interlocked microhook arrays with four different pitches (i.e., 25, 30, 35, and 40 μm) as functions of the swelling time.

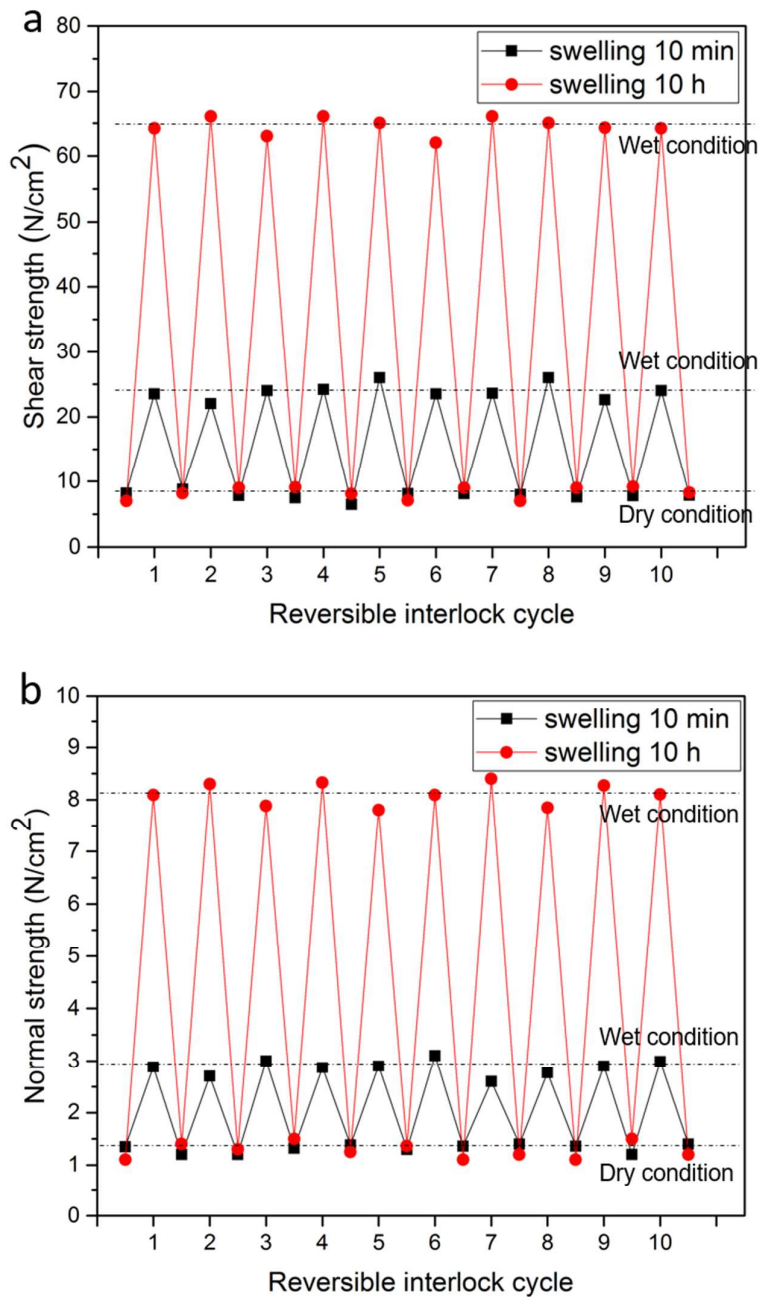


Figure S4. (a) Shear and (b) normal interlocking adhesion strengths during repeated swelling and deswelling cycles. For the durability tests, PEGDMA adhesives with a 30 μm pitch are swollen with water for two different times (i.e., 10 min and 10 h) followed by drying on a hot plate (30 $^{\circ}\text{C}$).

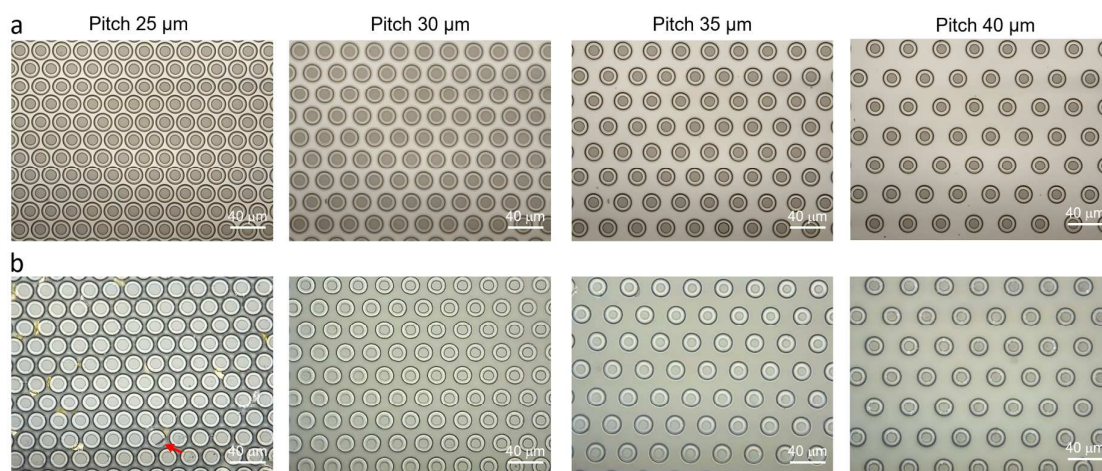


Figure S5. Optical microscope images of the PEGDMA microhook arrays with different pitches (a) before and (b) after 10 cycles of interlocking adhesion tests during repeated swelling and deswelling cycles. Slight tip deformations were observed with the microhook arrays with the smallest pitch of 25 μm (red arrow in Figure S5b).

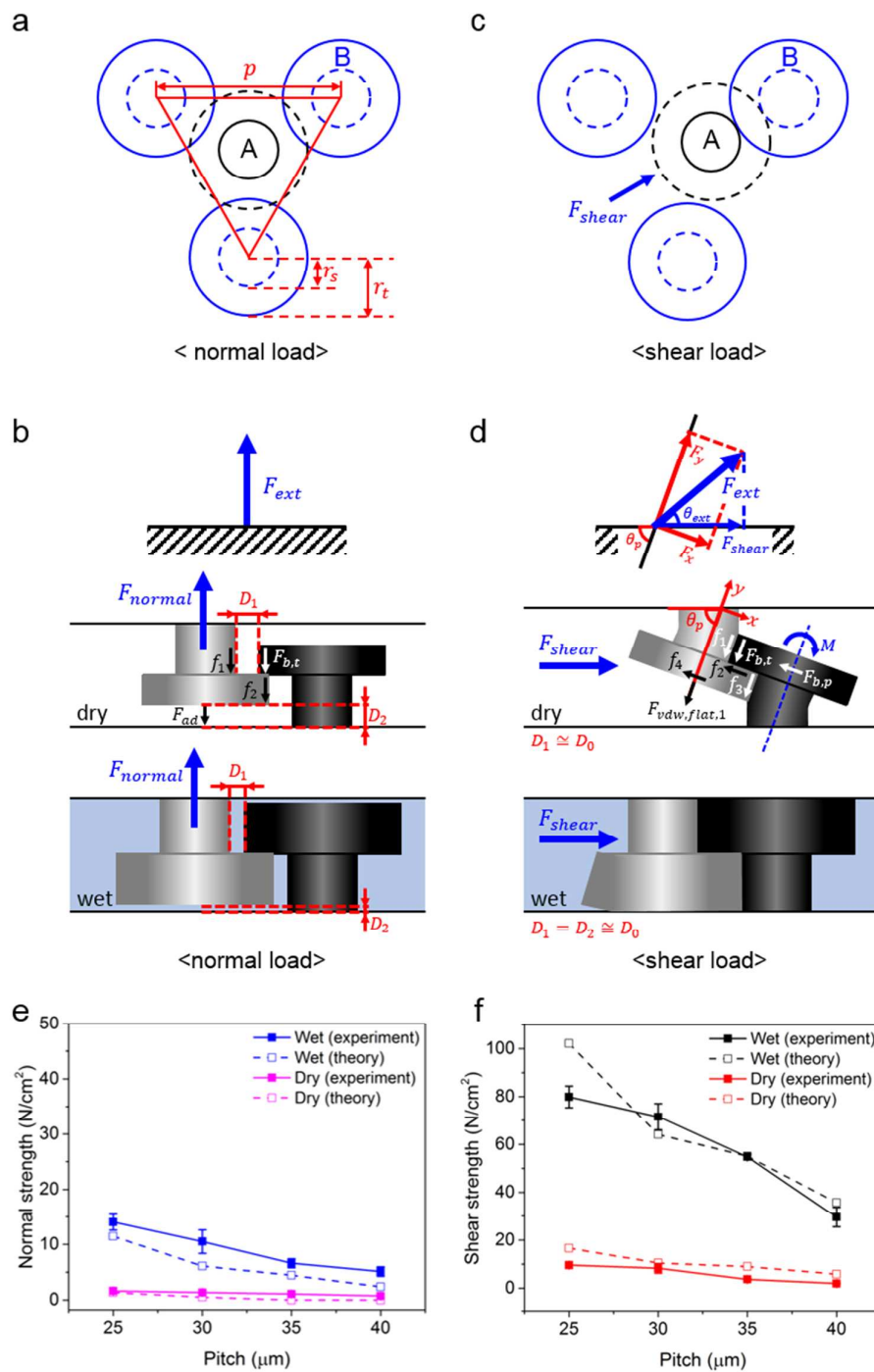


Figure S6. (a) Top and (b) side views of the model system of the interlocked microhooks under normal loading. (c) Top and (d) side views of the model system of the interlocked microhooks under shear loading. Plots of the measured (e) normal and (f) shear adhesion

strengths of the interlocked array with different pitches under the dry and wet conditions compared with the theoretical predictions.

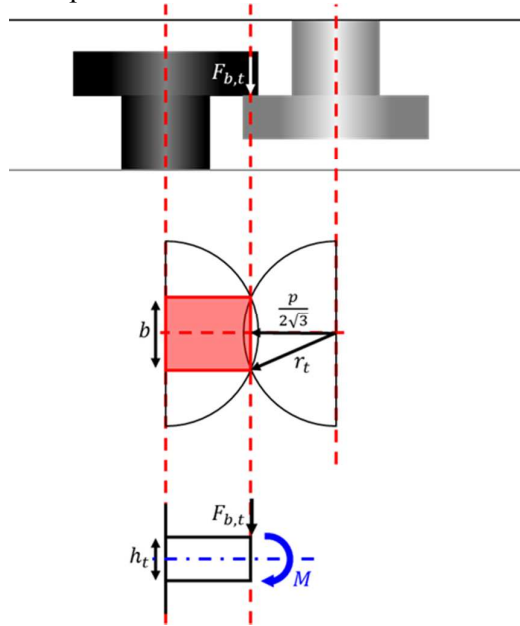


Figure S7. Schematic illustration describing the geometry of the tip and the bending force acting on the tip of the microhook ($F_{b,t}$).

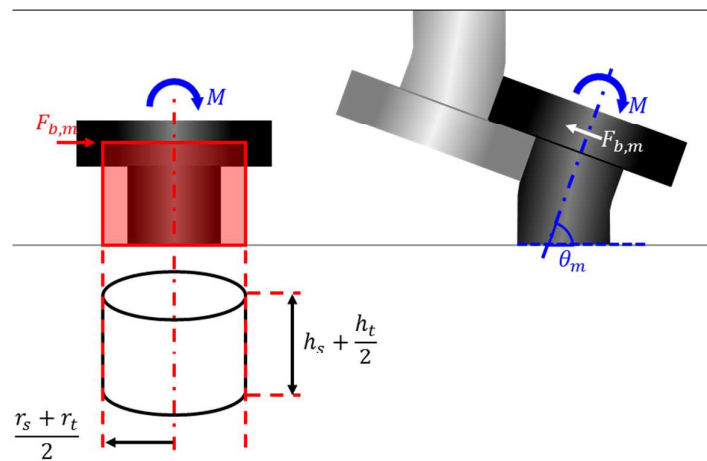
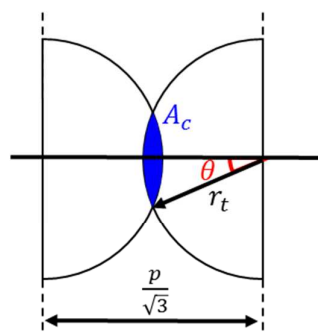


Figure S8. Schematic illustration describing the geometry of the microhooks and the bending force acting on the microhook ($F_{b,m}$).



$$\theta = \tan^{-1} \left(\sqrt{\frac{12r_t^2}{p^2} - 1} \right)$$

Figure S9. Schematic illustration describing the geometry of the tip–tip contact for the evaluation of the contact area (A_c) required for the calculation of $F_{vdw,tip}$.

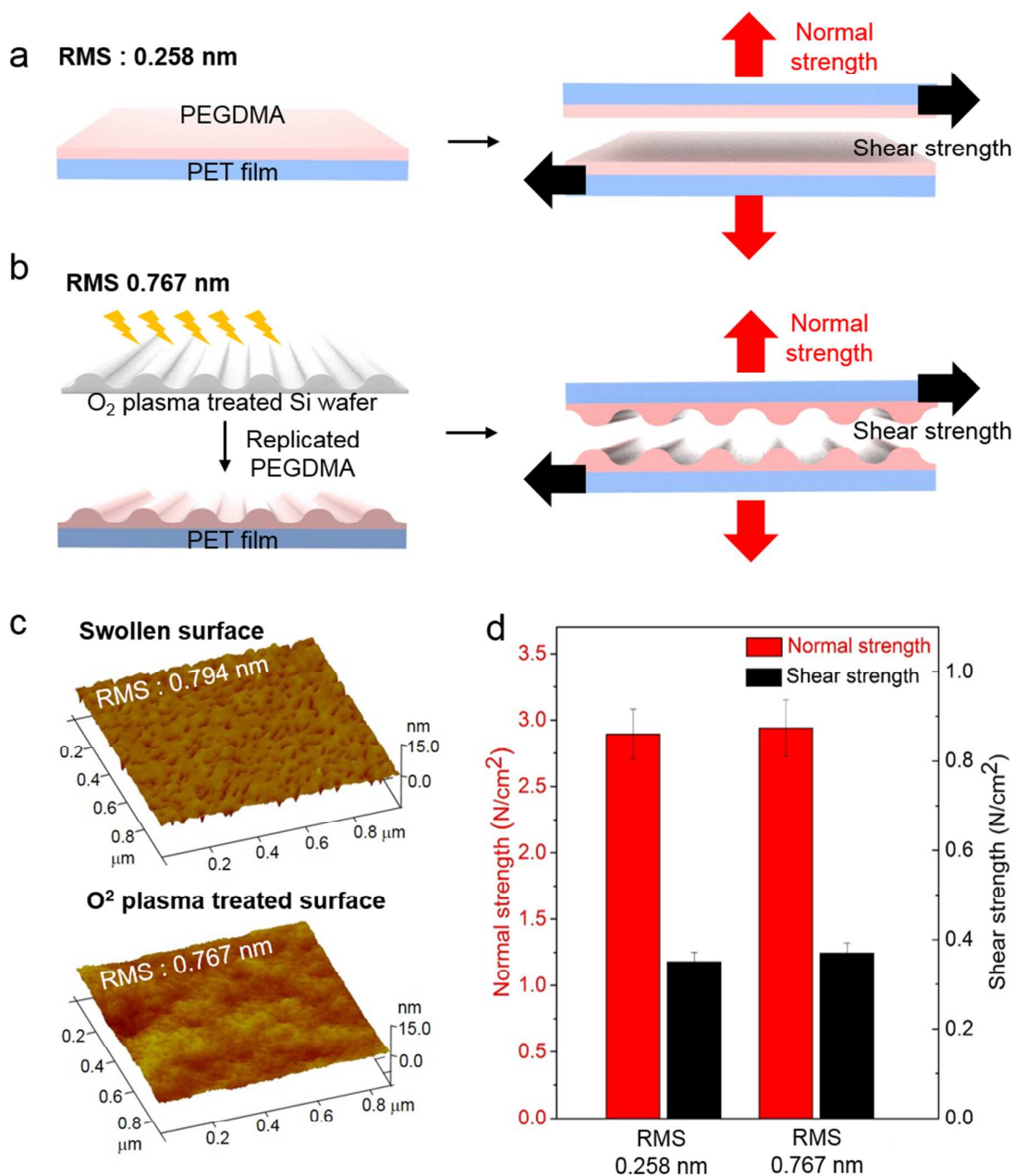


Figure S10. Schematic illustrations showing the normal and shear adhesion measurements using the PEGDMA adhesives with roughness of (a) ~ 0.258 nm and (b) ~ 0.767 nm. The measurements were performed in dry conditions. (c) RMS roughness values of the swollen PEGDMA film (top) and the PEGDMA film replicated from the plasma-treated Si wafer (bottom). (d) Normal and shear adhesion strengths of the PEGDMA films with the two different roughness values.

Reference

- (1) Leckband, D.; Israelachvili, J., Intermolecular forces in biology. *Q Rev Biophys.* **2001**, *34*, 105-267.
- (2) Alahmadi, A., Influence of triboelectrification on friction coefficient. *Int J Sci Eng Res.* **2014**, *5*, 32-39.
- (3) Mang, T., *Encyclopedia of Lubricants and Lubrication*. Springer Berlin Heidelberg: Berlin. 2014; pp 1998-2005.
- (4) Sokolnikoff, I. S., *Mathematical theory of elasticity*. TATA McGraw-Hill publishing company. Bombay, 1956; pp 100-107.
- (5) Dirks, J.-H., Physical principles of fluid-mediated insect attachment-Shouldn't insects slip? *Beilstein J Nanotech.* **2014**, *5*, 1160.